

## Little Known Characteristics of Phase Noise

by Paul Smith

### INTRODUCTION

There is a wealth of information available on the topic of phase noise, its characteristics<sup>1</sup>, how it can be measured<sup>2</sup>, and how it affects system performance<sup>3</sup>. It is well known that phase noise in oscillators and clocks becomes one of the limiting degradations in modern radio systems. However, most of the traditional analyses concentrate on degradations to sine wave signals in single carrier radio systems. The effects of phase noise on multicarrier receivers, wideband systems, or digital radios are very rarely discussed. This application note will address some of the rarely discussed issues related to phase noise in sampled data systems. It will focus primarily on multicarrier radios, wideband signals, and under-sampled radio architectures.

### PHASE JITTER IN SAMPLED DATA SYSTEMS

The easiest way to calculate the SNR degradations incurred by phase noise in a sampled data system is to convert phase noise to phase jitter. This is most easily accomplished by recognizing that a time delay is the same as a phase delay at a given frequency. Extending this concept and writing it in terms of noise power yields Equation 1.

$$\sigma_{\theta}^2 = \omega_{clk}^2 \sigma_t^2, \quad (1)$$

where  $\sigma_{\theta}$  = phase noise in rms radians  
 $\sigma_t$  = phase jitter in rms seconds  
 $\omega_{clk}$  = clock frequency in radians/sec

That is, for a given jitter error, a higher frequency signal will have more phase error. The term  $\sigma_{\theta}$  is the total integrated phase noise of the clock<sup>4</sup> and defines the clock SNR by

$$SNR_{clk}(dB) = -10 \log(\sigma_{\theta}^2) \quad (2)$$

Thus, Equation 1 relates the total integrated phase noise, or clock SNR, to the total jitter in the clock. Phase noise and clock jitter are two different ways to look at the same phenomenon.

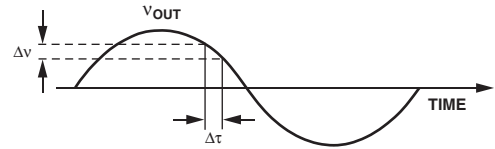


Figure 1.

Traditional sampled data SNR analyses use Figure 1 as an aid to determine how noise on a clock generates an error in the sampled data. From this it is seen that

$$\Delta v(t) = \Delta t \times v'_{out}(t)$$

$$E\{\Delta v^2(t)\} = E\{\Delta t^2 \times v'_{out}{}^2(t)\}$$

$$E\{\Delta v^2(t)\} = E\{\Delta t^2\} \times E\{v'_{out}{}^2(t)\},$$

zero mean, independence

Therefore,

$$\sigma_{err}^2 = \sigma_t^2 \times E\{v'_{out}{}^2(t)\},$$

where  $\sigma_t^2$  is in (rms seconds)<sup>2</sup>

From this it is seen that the noise power is a function of the jitter power and the power in the signal derivative.

The SNR of a signal sampled with a jittery clock is defined as

$$SNR_{sig} = \frac{\text{power in signal}}{\text{power in noise}} = \frac{\sigma_{out}^2}{\sigma_{err}^2} = \frac{1}{\sigma_t^2} \frac{E\{v_{out}{}^2(t)\}}{E\{v'_{out}{}^2(t)\}} \quad (3)$$

For example, in a single sine wave,

$$v_{out}(t) = A \sin \omega_O t$$

$$v'_{out}(t) = A \omega_O \cos \omega_O t$$

Therefore,

$$E\{v_{out}{}^2(t)\} = \text{power in } v_{out}(t) = \frac{A^2}{2}$$

$$E\{v'_{out}{}^2(t)\} = \text{power in } v'_{out}(t) = \frac{\omega_O^2 A^2}{2}$$

Using Equation 3,

$$SNR_{sig} = \frac{1}{\sigma_t^2} \frac{\frac{A^2}{2}}{\omega_o^2 \frac{A^2}{2}} = \frac{1}{\sigma_t^2} \frac{1}{\omega_o^2} \quad (4a)$$

$$SNR_{sig} = \frac{1}{4\pi^2 f_o^2 \sigma_t^2}, \text{ for a single carrier system.} \quad (4b)$$

This is the standard SNR equation for a single sine wave sampled by a clock with jitter and can be found in many publications<sup>5</sup>. Intuitively what is happening is that higher frequency signals have larger slew rates. This results in larger voltage changes as the sample time changes. It should be remembered that quantization noise and thermal noise must also be added to this to obtain the total noise out of a data converter.

Extending this to a multicarrier signal is a simple matter. Using the same procedure as before with  $v_{out}$  defined as a summation of n equal amplitude sine waves,

$$E\{v_{out}^2(t)\} = \frac{nA^2}{2}$$

$$E\{v'_{out}{}^2(t)\} = \frac{A^2(\omega_1^2 + \omega_2^2 + \dots + \omega_n^2)}{2}$$

$$SNR_{sig} = \frac{1}{\sigma_t^2} \frac{\frac{nA^2}{2}}{A^2(\omega_1^2 + \omega_2^2 + \dots + \omega_n^2)} =$$

$$\frac{1}{\sigma_t^2} \frac{n}{(\omega_1^2 + \omega_2^2 + \dots + \omega_n^2)} = \frac{n}{4\pi^2 \sigma_t^2 \sum_n f_i^2}$$

This is relative to the entire signal,  $v_{out}$ . When referenced to only one of the carriers, the SNR becomes

$$SNR_{sig} = \frac{1}{4\pi^2 \sigma_t^2 \sum_n f_i^2}, \quad (5)$$

for a single carrier in a multicarrier system.

Compared to the single carrier case, Equation 4b, the denominator has n more frequency terms. The SNR on a per carrier basis (i.e., dBc) has been degraded by approximately  $10 \log(n)$ . However, in a data converter each carrier may need to be reduced by  $10 \log(n)$  to  $20 \log(n)$ , depending on signal statistics, in order to keep from clipping the quantizer. This, in effect, raises the quantization and thermal noise floor by up to  $20 \log(n)$ . Thus, jitter may contribute less to the overall SNR than in the single carrier case. Quantization and thermal noise may become more dominant.

Many modern radio systems don't use narrow-band carriers. Modulated data often occupies a fairly wide spectrum. In order to determine how clock jitter effects the SNR for such systems, it is convenient to assume the data has zero mean and a flat spectrum uniformly distributed between  $f_L$  and  $f_H$ ,  $f_L < f_H$  as shown in Figure 2. When squared and integrated over its bandwidth, the total signal power  $\sigma_{out}^2$  is obtained.

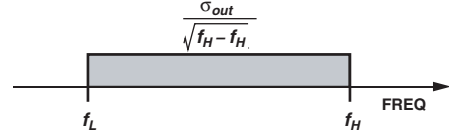


Figure 2.

One form of Parseval's theorem states that the power of a signal in the time domain equals the power of the signal in the frequency domain. That is,

$$\int_{-\infty}^{+\infty} |v(t)|^2 dt = \frac{1}{2\pi} \int_{-\infty}^{+\infty} |g(\omega)|^2 d\omega = \int_{-\infty}^{+\infty} |g(f)|^2 df$$

where  $|g(f)|^2$  is the power spectral density in Watt/Hz.

In addition, using the differentiation theorem of the Fourier transform, which states that the Fourier transform of a derivative is just the Fourier transform of the original function multiplied by  $i\omega$ , as shown below,

$$\mathfrak{F}\{v'(t)\} = i\omega \mathfrak{F}\{v(t)\}$$

and combining this with Parseval's theorem, it is seen that the power in  $v'(t)$  is the same as the power in  $i\omega g(\omega)$ , as described below,

$$\int_{-\infty}^{+\infty} (v'(t))^2 dt = \frac{1}{2\pi} \int_{-\infty}^{+\infty} |i\omega g(\omega)|^2 d\omega =$$

$$\frac{1}{2\pi} \int_{-\infty}^{+\infty} \omega^2 |g(\omega)|^2 d\omega = \int_{-\infty}^{+\infty} (2\pi f)^2 |g(f)|^2 df$$

For  $g(f) = \frac{\sigma_{out}}{\sqrt{f_H - f_L}}$  only between  $f_L$  and  $f_H$  (and zero everywhere else), this becomes

$$E\{v'_{out}(t)^2\} = \int_{f_L}^{f_H} (2\pi f)^2 \frac{\sigma_{out}^2}{(f_H - f_L)} df$$

$$E\{v'_{out}(t)^2\} = \frac{\sigma_{out}^2}{f_H - f_L} \int_{f_L}^{f_H} (2\pi f)^2 df$$

$$E\{v'_{out}(t)^2\} = \frac{4\pi^2 (f_H^3 - f_L^3) \sigma_{out}^2}{3(f_H - f_L)} = \frac{4\pi^2 (f_H^2 + f_H f_L + f_L^2) \sigma_{out}^2}{3}$$

Using Equation 3,

$$SNR_{sig} = \frac{1}{\sigma_t^2} \frac{3}{(f_H^2 + f_H f_L + f_L^2)}$$

This is the SNR resulting from a flat, wideband signal between  $f_L$  and  $f_H$  being sampled by a clock with jitter  $\sigma_t$ . As a sanity check, setting  $f_L = f_H = f_O$  (i.e., all the power resides in a single frequency term  $f_O$ ) results in the same expression as Equation 4b for the single frequency case.

An alternative expression is obtained by letting  $f_L = f_O - BW/2$  and  $f_H = f_O + BW/2$ . For this case the expression becomes

$$SNR_{sig} = \frac{1}{4\pi^2\sigma_t^2\left(f_O^2 + \frac{BW^2}{12}\right)}, \quad (6)$$

for a flat signal centered at  $f_O$  having bandwidth  $BW$ .

Again, as a sanity check, when  $BW=0$  the result matches the single carrier case in Equation 4b.

A consequence of all this math is that as long as  $f_O > 10BW$ , the bandwidth of the signal can probably be neglected. Treating the modulated signal as a single carrier will give virtually equal results. However, if this is not true, then using the single carrier approximation will give results that are too optimistic.

This entire discussion has focused on sampled data systems, but the effects of aliasing have not been mentioned. All of the equations derived above assume there is no aliasing. The bandwidth of the jitter is considered to fall entirely (and conveniently) into a single Nyquist zone. If the jitter is bad enough, and the signal close enough to a Nyquist edge, the noise caused by jitter can alias back in band, degrading SNR even further. This effect is illustrated in Figure 3. A similar problem exists with clock feedthrough. If the signal is close to the clock, phase noise from the clock can directly leak to the output, degrading the noise floor.

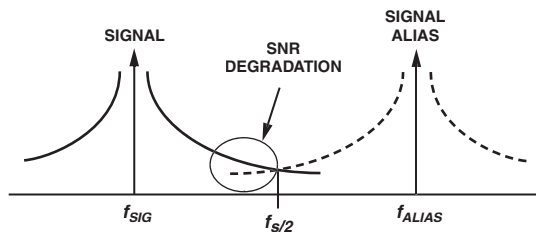


Figure 3.

### PHASE NOISE IN SAMPLED DATA SYSTEMS

In addition, nowhere in the preceding discussion did the spectrum of the clock phase noise come into play. All that was considered was the total jitter (in rms seconds) which was calculated from the total integrated phase noise using Equation 1. To see how the phase noise spectrum of the clock affects the sampled data spectrum, it is most convenient to use a single sine wave signal. Combining Equation 1 with 4a yields Equation 7a.

$$SNR_{sig} = \frac{1}{\sigma_\theta^2} \left( \frac{f_{clk}}{f_{sig}} \right)^2 \quad (7a)$$

Using Equation 2, this can be written as

$$SNR_{sig} = SNR_{clk} \left( \frac{f_{clk}}{f_{sig}} \right)^2 \quad (7b)$$

The SNR of the resulting sampled signal is the same as the SNR of the clock but scaled by the clock and signal frequency ratio. As the signal frequency gets higher, the SNR degrades in a 20 log fashion. This illustrates why undersampled systems (i.e., one in which the signal frequency occupies one of the higher Nyquist bands) require clocks with much better phase jitter than baseband systems. In fact, performance in IF-sampling digital radio architectures are often limited by clock phase noise, not data converter performance.

Although not apparent from Equation 7b, the spectral shape of the clock phase noise is superimposed on the sampled data, as illustrated in Figure 3. This can intuitively be seen by modeling the sampling process with a mixer. As shown in Figure 4, when a clock with phase noise  $\theta$  is applied to a mixer, the output contains two mixing products, each of which contains the full phase noise  $\theta$  of the clock. Although this simplistic model does not show the scaling factor described in Equation 7, it is useful to show how the phase spectrum of the clock shows up on the resulting signal.

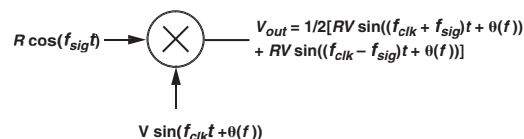


Figure 4.

This can easily be tested by phase modulating a clock and feeding it into an ADC. By applying different signal frequencies, Equation 7 can also be verified. An AD9430 ADC was clocked at 61.44 MHz with a clock phase modulated such that the first sidebands were  $-60$  dBc. Figures 5a, 5b, and 5c show the results of the experiment.

Figure 5a shows the results with a 3.84 MHz input. The clock modulation components can be seen as the two small spurs clustered close to the signal fundamental. According to Equation 7, the clock modulation spurs should be  $-60 - 20 \log(61.44/3.86) = -84$  dBc. The results in Figure 5a are quite close to this number.

Figure 5b shows the results with a 65.28 MHz input. This is in the 3rd Nyquist zone. The FFT shows the baseband alias in the same location as the 3.84 MHz signal in Figure 5a (i.e.,  $65.28 \text{ MHz} - 61.44 \text{ MHz} = 3.84 \text{ MHz}$ ). Here  $f_{clk} \sim f_{sig}$  and the  $-60$  dBc clock spurs can readily be seen superimposed on the signal, also at  $-60$  dBc. This is to be expected according to Equation 7b.

Figure 5c shows the results with a 124.72 MHz input in the 5th Nyquist zone. This frequency is about twice that of Figure 5b and according to Equation 7 the spurs should increase about 6 dB, which is what is seen.

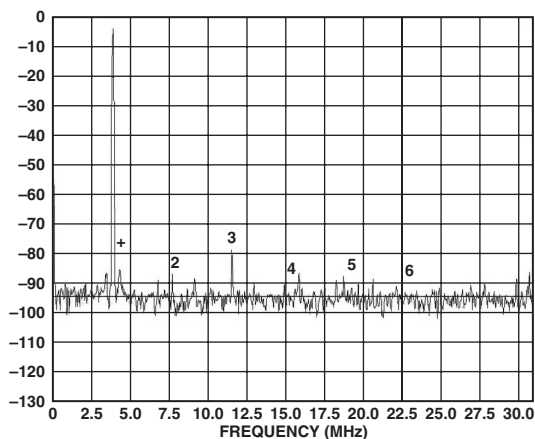


Figure 5a.

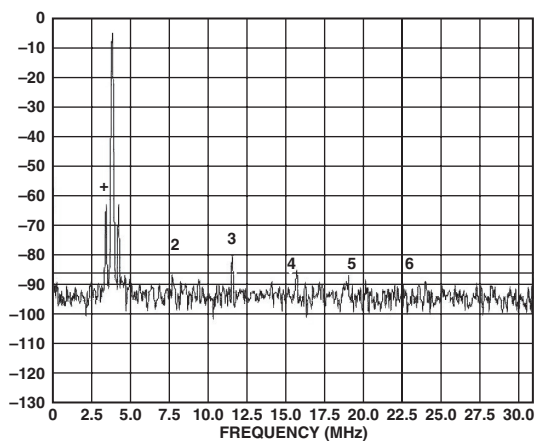


Figure 5b.

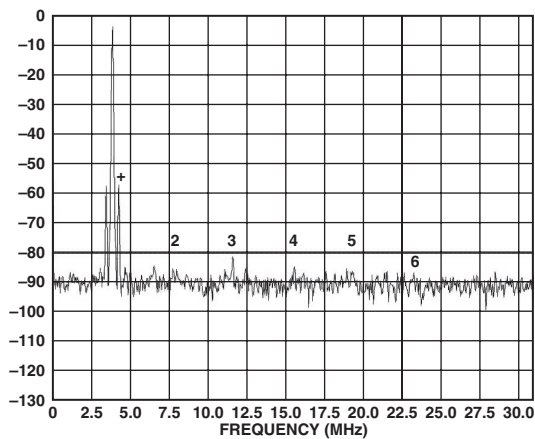


Figure 5c.

Thus, it appears the clock spectrum does indeed appear around the sampled signal with a scaling factor described by Equation 7. However, so far, all of the preceding discussions have not differentiated between ADCs and DACs. Do DACs exhibit the same characteristic seen by ADCs? A similar experiment was run on an AD9744 DAC using a 61.44 MHz clock phase modulated to give -40 dBc sidebands, generating an 11 MHz sine wave. The results over five Nyquist bands are shown in Figure 6.

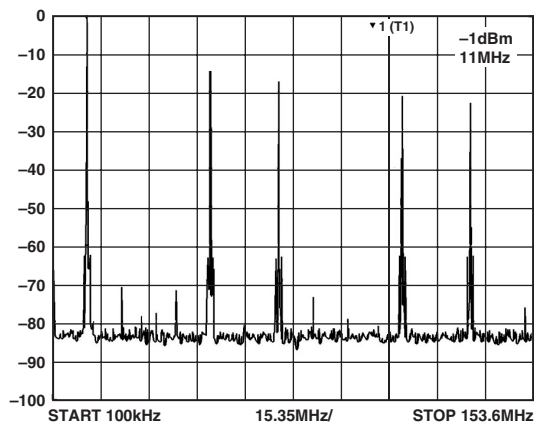


Figure 6.

The Sinc function inherent in DAC outputs can clearly be seen. But what is happening with the clock spurs? These are clearly seen at each of the output images but the amplitudes don't increase as they did with the ADC. Relative to full scale, the spur amplitudes remain constant.

There are several ways to look at this. When viewed in dBc, as the signal frequency goes up, the modulation spurs get worse in the same manner as described by Equation 7b. The Sinc function applies to both the signal amplitude and the induced clock phase noise. Calculating the spur amplitude relative to each carrier (i.e., in dBc), Equation 7b is a good description.

Alternatively, the Sinc characteristic is defined as

$$\frac{\sin\left(\frac{\pi f_{sig}}{f_{clk}}\right)}{\frac{\pi f_{sig}}{f_{clk}}}$$

The amplitude of the noise is given by the reciprocal of Equation 7a.

$$\frac{N}{S} = \sigma_{\theta}^2 \left(\frac{f_{sig}}{f_{clk}}\right)^2$$

That is, the noise is directly proportional to clock phase

noise and signal frequency. Squaring the Sinc function (because *power* spectral densities are being examined) and multiplying these two to get a composite noise transfer function out of the DAC yields

$$\frac{N}{S} = \sigma_{\theta}^2 \frac{\sin^2\left(\frac{\pi f_{sig}}{f_{clk}}\right)}{\pi^2}$$

The periodic nature of the nulls caused by the sinusoid still exist. However, the denominator of the Sinc function is what causes the roll-off at higher frequencies. This attenuation has been exactly cancelled by the increasing phase noise at higher frequencies described by Equation 7b. Thus, the phase noise out of a DAC will not grow at higher frequencies.

#### APPLICATION TO SYSTEM DEBUGGING

Besides the obvious issues revolving around designing systems to minimize signal degradations, there are several other consequences to these results worth mentioning. These are related to finding the source of mystery spurs and noise. For instance, if the noise floor rises at the DAC output, it is most likely not caused by clock phase noise. It may be digital coupling into the output circuitry.

If a spur exists in a sampled signal, a good test to see if it comes from the clock is to change the signal amplitude. Analog distortion terms will change at twice (2nd order distortion) or three times (3rd order distortion) the rate of the signal amplitude change. Spurs due to nonlinearity in the quantizer may not change at all, or if they do change, they will change unpredictably, when the signal amplitude changes. On the other hand, spurs due to the clock will change dB for dB with the signal.

When trying to identify the source of a spur in a sampled data signal, look not only at the explicit spur frequency, which could be caused by a signal directly coupling into the output, but also at the frequency offset from the

signal. For example, if a spur is 10MHz away from the carrier, look to see if there is a 10MHz oscillator somewhere in the system. If so, this frequency is most likely leaking in through the clock.

#### SUMMARY

This application note examined the relationship between phase noise and jitter, deriving the SNR degradations that occur when a signal is sampled by a clock with jitter. The results were extended to multicarrier and wideband modulated data systems. Clock phase noise spectral issues were then dealt with, examining the resulting spectrum at the output of ADCs and DACs. Finally, the results are applied to debugging a system that may have unusual spurs that would otherwise be unaccounted for.

#### NOTES

<sup>1</sup>W. P. Robins, *Phase Noise in Signal Sources* (London: Peter Peregrinus Ltd., 1982).

<sup>2</sup>"Understanding and Measuring Phase Noise in the Frequency Domain," Hewlett Packard, Application Note 207, 1976.

<sup>3</sup>Stanley J. Goldman, *Phase Noise Analysis in Radar Systems Using Personal Computers* (New York: John Wiley & Sons, 1989).

<sup>4</sup>"VCO Phase Noise," Mini-Circuits, Application Note #2.

<sup>5</sup>"Linear Design Seminar," Analog Devices, Inc., Norwood, MA, 1995, pp. 5-20.





